

1
2
3
4
5
6
7
8
9
10
11
12
13
14
15
16
17
18
19
20
21
22
23
24
25
26
27
28
29
30
31
32

Human genetic analyses of organelles highlight the nucleus in age-related trait heritability

Rahul Gupta^{1,2,3}, Konrad J. Karczewski^{2,3}, Daniel Howrigan^{2,3}, Benjamin M. Neale^{2,3,*}, Vamsi K. Mootha^{1,2,*}

¹ Howard Hughes Medical Institute and Department of Molecular Biology, Massachusetts General Hospital, Boston, MA 02114

² Broad Institute of MIT and Harvard, Cambridge, MA 02142

³ Analytic and Translational Genetics Unit, Center for Genomic Medicine, Massachusetts General Hospital, Boston, MA 02114, USA

*Corresponding authors: bneale@broadinstitute.org (B.M.N.), vamsi@hms.harvard.edu (V.K.M.)

Keywords: mitochondria, nucleus, aging, oxidative phosphorylation, OXPHOS, transcription factor, zinc finger, KRAB domain, gene regulation, UK Biobank, constraint, dominance, haplosufficiency, haplosufficient, PPARGC1A, ESRRA, TFAM

33 **Abstract**

34 Most age-related human diseases are accompanied by a decline in cellular organelle integrity, including
35 impaired lysosomal proteostasis and defective mitochondrial oxidative phosphorylation. An open
36 question, however, is the degree to which inherited variation in or near genes encoding each organelle
37 contributes to age-related disease pathogenesis. Here, we evaluate if genetic loci encoding organelle
38 proteomes confer greater-than-expected age-related disease risk. As mitochondrial dysfunction is a
39 “hallmark” of aging, we begin by assessing nuclear and mitochondrial DNA loci near genes encoding the
40 mitochondrial proteome and surprisingly observe a lack of enrichment across 24 age-related traits. Within
41 nine other organelles, we find no enrichment with one exception: the nucleus, where enrichment
42 emanates from nuclear transcription factors. In agreement, we find that genes encoding several
43 organelles tend to be “haplosufficient,” while we observe strong purifying selection against heterozygous
44 protein-truncating variants impacting the nucleus. Our work identifies common variation near
45 transcription factors as having outsize influence on age-related trait risk, motivating future efforts to
46 determine if and how this inherited variation then contributes to observed age-related organelle
47 deterioration.

48

49 **Introduction**

50 The global burden of age-related diseases such as type 2 diabetes (T2D), Parkinson’s disease (PD), and
51 cardiovascular disease (CVD) has been steadily rising due in part to a progressively aging population. These
52 diseases are often highly heritable: for example, narrow-sense heritabilities were recently estimated as
53 56% for T2D, 46% for general hypertension, and 41% for atherosclerosis¹. Genome-wide association
54 studies (GWAS) have led to the discovery of thousands of robust associations with common genetic
55 variants², implicating a complex genetic architecture as underlying much of the heritable risk. These loci
56 hold the potential to reveal underlying mechanisms of disease and spotlight targetable pathways.

57 Aging has been associated with dysfunction in many cellular organelles³. Dysregulation of autophagic
58 proteostasis, for which the lysosome is central, has been implicated in myriad age-related disorders
59 including neurodegeneration, heart disease, and aging itself⁴, and mouse models deficient for autophagy
60 in the central nervous system show neurodegeneration^{5,6}. Endoplasmic reticular (ER) stress has been
61 invoked as central to metabolic syndrome and insulin resistance in T2D⁷. Disruption in the nucleus through
62 increased gene regulatory noise from epigenetic alterations³ and elevated nuclear envelope “leakiness”⁸
63 has been implicated in aging. Dysfunction in the mitochondria has even been invoked as a “hallmark” of
64 aging³ and has been observed in many common age-associated diseases^{9–15}. In particular, deficits in
65 mitochondrial oxidative phosphorylation (OXPHOS) have been documented in aging and age-related
66 diseases as evidenced by *in vivo* ³¹P-NMR measures^{10,16}, enzymatic activity^{11,12,17–21} in biopsy material,
67 accumulation of somatic mitochondrial DNA (mtDNA) mutations^{13,14,22}, and a decline in mtDNA copy
68 number (mtCN)¹⁵.

69 Given that a decline in organelle function is observed in age-related disease, a natural question is whether
70 inherited variation in loci encoding organelles is enriched for age-related disease risk. Though it has long
71 been known that recessive mutations leading to defects within many cellular organelles can lead to
72 inherited syndromes (e.g., mutations in >300 nuclear DNA (nucDNA)-encoded mitochondrial genes lead
73 to inborn mitochondrial disease²³), it is unknown how this extends to common disease. In the present
74 study, we use a human genetics approach to assess common variation in loci relevant to the function of
75 ten cellular organelles. We begin with a deliberate focus on mitochondria given the depth of literature
76 linking it to age-related disease, interrogating both nucDNA and mtDNA loci that contribute to the
77 organelle’s proteome. This genetic approach is supported by the observation that heritability estimates
78 of measures of mitochondrial function are substantial (33–65%^{24,25}). We then extend our analyses to nine
79 additional organelles.

80 To our surprise, we find no evidence of enrichment for genome-wide association signal in or near
81 mitochondrial genes across any of our analyses. Further, of ten tested organelles, only the nucleus shows
82 enrichment among many age-associated traits, with the signal emanating from the transcription factors
83 (TFs). Further analysis shows that genes encoding the mitochondrial proteome tend to be tolerant to
84 heterozygous predicted loss-of-function (pLoF) variation and thus are surprisingly “haplosufficient” – i.e.,
85 show little fitness cost with heterozygous pLoF. In contrast, nuclear TFs are especially sensitive to gene
86 dosage and are often “haploinsufficient”, showing substantial purifying selection against heterozygous
87 pLoF. Thus, our work highlights inherited variation influencing gene-regulatory pathways, rather than
88 organelle physiology, in the inherited risk of common age-associated diseases.

89 **Results**

90 **Age-related diseases and traits show diverse genetic architectures**

91 To systematically define age-related diseases, we turned to recently published epidemiological data from
92 the United Kingdom (U.K.)²⁶ in order to match the U.K. Biobank (UKB)²⁷ cohort. We prioritized traits whose
93 prevalence increased as a function of age (**Methods**) and were represented in UKB
94 (https://github.com/Nealelab/UK_Biobank_GWAS) and/or had available published GWAS meta-

95 analyses^{28–37} (**Figure 1A, Supplementary note**). We used SNP-heritability estimates from stratified linkage
 96 disequilibrium score regression (S-LDSC, <https://github.com/bulik/ldsc>)³⁸ to ensure that our selected traits
 97 were sufficiently heritable (**Table S1, Methods, Supplementary note**), observing heritabilities across UKB
 98 and meta-analysis traits as high as 0.28 (bone mineral density), all with heritability Z-score > 4. We then
 99 computed pairwise genetic and phenotypic correlations between the age-associated traits to compare
 100 their respective genetic architectures and phenotypic relationships (**Figure 1B, Table S2, Methods**). In
 101 general, genetic correlations were greater in magnitude than respective phenotypic correlations,

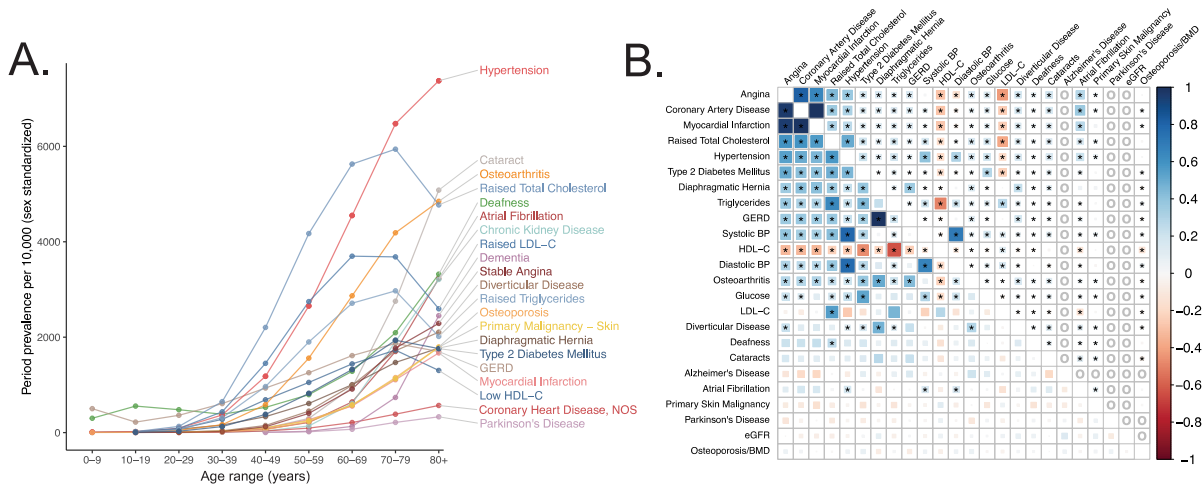


Figure 1. Selection of genetically diverse age-related diseases and traits using epidemiological data. **A.** Period prevalence of age-associated diseases systematically selected for this study (**Methods**). Epidemiological data obtained from Kuan et al. 2019. **B:** Genetic (lower half) and phenotypic (upper half) correlation between the selected age-related traits. All correlations were assessed between UK Biobank phenotypes with the exception of eGFR, Alzheimer's Disease, and Parkinson's Disease, for which the respective meta-analyses were used (**Methods**). Grey "o" in phenotypic correlations indicate phenotypes not tested within UKB for which individual-level data was not available. Point estimates and standard errors/p-values reported in **Table S2**. * represents correlations that are significantly different from 0 at a Bonferroni-corrected threshold for $p = 0.05$ across all tested traits.

102 potentially as GWAS are less sensitive to purely non-genetic factors that influence phenotype (e.g.,
 103 measurement error). As expected we find a highly correlated module of primarily cardiometabolic traits
 104 with high density lipoprotein (HDL) showing anti-correlation³⁹. Interestingly, several other traits
 105 (gastroesophageal reflux disease (GERD), osteoarthritis) showed moderate genetic correlation to the
 106 cardiometabolic trait cluster while atrial fibrillation, for which T2D and CVD are risk factors⁴⁰, showed
 107 phenotypic, but not genetic, correlation. Our final set of prioritized, age-associated traits included 24
 108 genetically diverse, heritable phenotypes (**Table S1**). Of these, 11 traits were sufficiently heritable only in
 109 UKB, 3 were sufficiently heritable only among non-UKB meta-analyses, and 10 were well-powered in both
 110 UKB and an independent cohort.

111
 112 **Mitochondrial genes are not enriched among age-related trait GWAS**

113 To test if age-related trait heritability was enriched among mitochondria-relevant loci, we began by simply
 114 asking if ~1100 nucDNA genes encoding the mitochondrial proteome from the MitoCarta2.0 inventory⁴¹
 115 were found near lead SNPs for our selected traits represented in the NHGRI-EBI GWAS Catalog
 116 (<https://www.ebi.ac.uk/gwas/>)⁴² more frequently than expectation (**Methods, Supplementary note**). To
 117 our surprise, no traits showed a statistically significant enrichment of mitochondrial genes (**Figure 2-S1A**);
 118 in fact, six traits showed a statistically significant depletion. Even more strikingly, MitoCarta genes tended
 119 to be nominally enriched in fewer traits than the average randomly selected sample of protein-coding
 120 genes (**Figure 2-S1B**, empirical $p = 0.014$). This lack of enrichment was observed more broadly across
 121 virtually all traits represented in the GWAS Catalog (**Figure 2-S1C**). We also examined specific

122 transcriptional regulators of mitochondrial biogenesis (*TFAM*, *GABPA*, *GABPB1*, *ESRRA*, *YY1*, *NRF1*,
 123 *PPARGC1A*, *PPARGC1B*) and found very little evidence supporting a role for these genes in modifying risk
 124 for the age-related GWAS Catalog phenotypes (**Supplementary note**).

125 To investigate further, we turned to U.K. Biobank (UKB). We compiled and tested loci encoding the
 126 mitochondrial proteome (**Figure 2A**) with which we interrogated the association between common
 127 mitochondrial variation and common disease. First, we considered all common variants in or near nucDNA
 128 MitoCarta genes, as well as two subsets of MitoCarta: mitochondrial Mendelian disease genes²³ and
 129 nucDNA-encoded OXPPOS genes. Second, we obtained and tested mtDNA genotypes at up to 213 loci
 130 after quality control (**Methods**) from 360,662 individuals for associations with age-related traits.

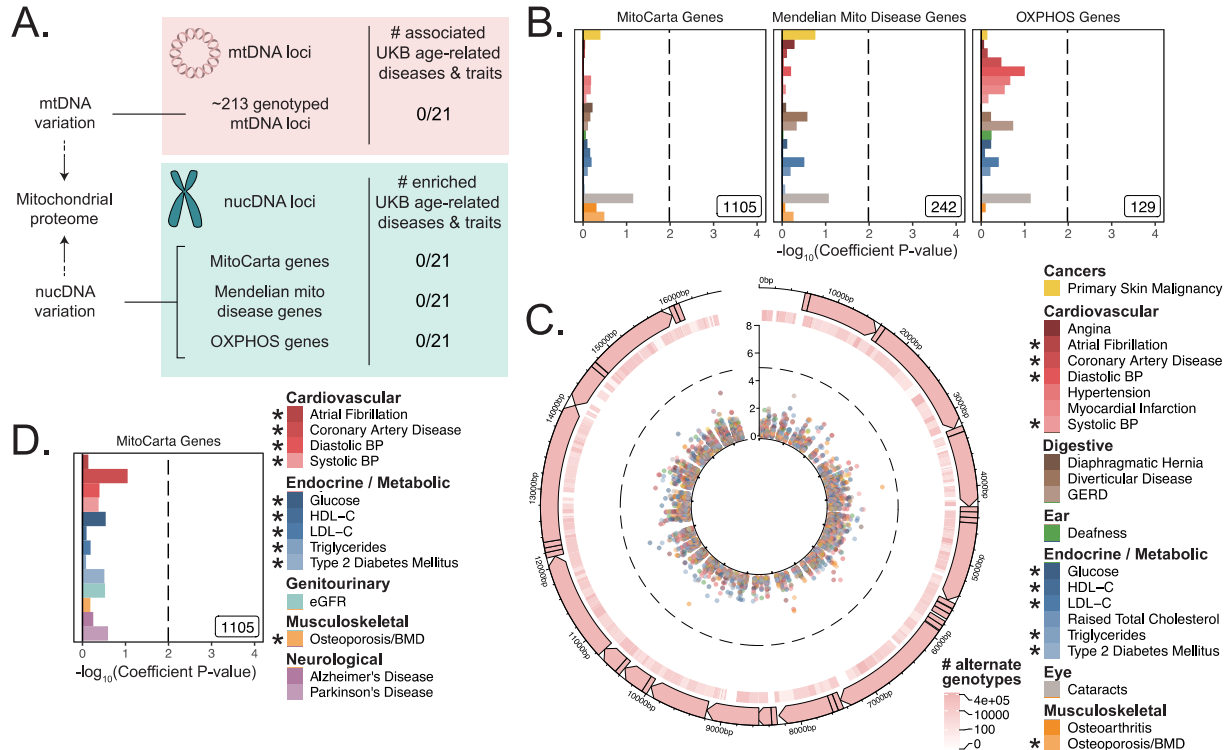


Figure 2. Assessment of the association of nucDNA and mtDNA loci contributing to the mitochondrial proteome with age-related traits. **A.** Scheme outlining the aspects of mitochondrial function assessed in this study. nucDNA loci contributing to the mitochondrial proteome are shown in teal, while mtDNA loci are shown in pink. **B.** S-LDSC enrichment p-values on top of the baseline model in UKB. Inset labels represent gene-set size; dotted line represents BH FDR 0.1 threshold. **C.** Visualization of mtDNA variants and associations with age-related diseases. The outer-most track represents the genetic architecture of the circular mtDNA. The heatmap track represents the number of individuals with alternate genotype on log scale. The inner track represents mitochondrial genome-wide association p-values, with radial angle corresponding to position on the mtDNA and magnitude representing $-\log_{10} P$ value. Dotted line represents Bonferroni cutoff for all tested trait-variant pairs. **D.** Replication of S-LDSC enrichment results in meta-analyses. Dotted line represents BH FDR 0.1 threshold. * represents traits for which sufficiently well powered cohorts from both UKB and meta-analyses were available. The trait color legend to the right of panel **C** applies to panels **B** and **C**, representing UKB traits.

131 First, we used S-LDSC^{38,43} and MAGMA (<https://ctg.cncr.nl/software/magma>)⁴⁴, two robust methods that
 132 can be used to assess gene-based heritability enrichment accounting for LD and several confounders, to
 133 test if there was any evidence of heritability enrichment among MitoCarta genes (**Methods**). We found
 134 no evidence of enrichment near nucDNA MitoCarta genes for any trait tested in UKB using S-LDSC (**Figure**
 135 **2B**, **2-S7A**), consistent with our results from the GWAS Catalog. We replicated this lack of enrichment
 136 using MAGMA at two different window sizes (**Figure 2-S7C**, **2-S7E**; all $q > 0.1$).

137 Given the lack of enrichment among the MitoCarta genes, we wanted to (1) verify that our selected
138 methods could detect previously reported enrichments and (2) confirm that common variation in or near
139 MitoCarta genes can lead to expression-level perturbations. We first successfully replicated previously
140 reported enrichment among tissue-specific genes for key traits using both S-LDSC (**Figure 2-S2, 2-S3**) and
141 MAGMA (**Figure 2-S4, 2-S5, Supplementary note, Methods**). We next confirmed that we had sufficient
142 power using both S-LDSC and MAGMA to detect physiologically relevant enrichment effect sizes among
143 MitoCarta genes (**Figure 2-S6, Methods, Supplementary note**). We finally examined the landscape of cis-
144 expression QTLs (eQTLs) for these genes and found that almost all MitoCarta genes have cis-eQTLs in at
145 least one tissue and often have cis-eQTLs in more tissues than most protein-coding genes (**Figure 2-S8,**
146 **Methods, Supplementary note**). Hence, our selected methods could detect physiologically relevant
147 heritability enrichments among our selected traits at gene-set sizes comparable to that of MitoCarta, and
148 common variants in or near MitoCarta genes exerted *cis*-control on gene expression.

149 Next, we considered mtDNA loci genotyped in UKB, obtaining calls for up to 213 common variants passing
150 quality control across 360,662 individuals (**Methods, Supplementary note**). We found no significant
151 associations on the mtDNA for any of the 21 age-related traits available in UKB using linear or logistic
152 regression (**Methods, Figure 2C, 2-S9, Table S4**).

153 As a control and to validate our approach, we also performed mtDNA-GWAS for specific traits with
154 previously reported associations. A recent analysis of ~147,437 individuals in BioBank Japan revealed four
155 distinct traits with significant mtDNA associations⁴⁵. Of these, creatinine and aspartate aminotransferase
156 (AST) had sufficiently large sample sizes in UKB. We observed a large number of associations throughout
157 the mtDNA for both traits ($p < 1.15 * 10^{-5}$, **Figure 2-S9E**). Thus, our mtDNA association method was able
158 to replicate robust mtDNA associations among well-powered traits.

159 We sought to replicate our negative results in an independent cohort. We turned to published GWAS
160 meta-analyses²⁸⁻³⁷ (**Table S1**) and successfully replicated the lack of enrichment for MitoCarta genes
161 across all 10 traits with an available independent cohort GWAS using S-LDSC (**Figure 2D, 2-S7B**) and
162 MAGMA at two different window sizes (**Figure 2-S7D, Supplementary note**; all $q > 0.1$). Importantly, while
163 we were unable to pursue analyses for PD and Alzheimer's disease in UKB due to limited case counts, we
164 tested MitoCarta genes among well-powered meta-analyses for these disorders (**Supplementary note**)
165 and observed no enrichment (**Figure 2D**; all $q > 0.1$).

166 In summary, we tested (1) nucDNA loci near genes that encode the mitochondrial proteome in the GWAS
167 Catalog, UKB, and GWAS meta-analyses, (2) transcriptional regulators of mitochondrial biogenesis in the
168 GWAS Catalog, and (3) mtDNA variants in UKB. We found no convincing evidence of heritability
169 enrichment for common age-associated diseases near these mitochondrial loci.

170

171 **Of all tested organelles, only the nucleus shows enrichment for age-related trait heritability**

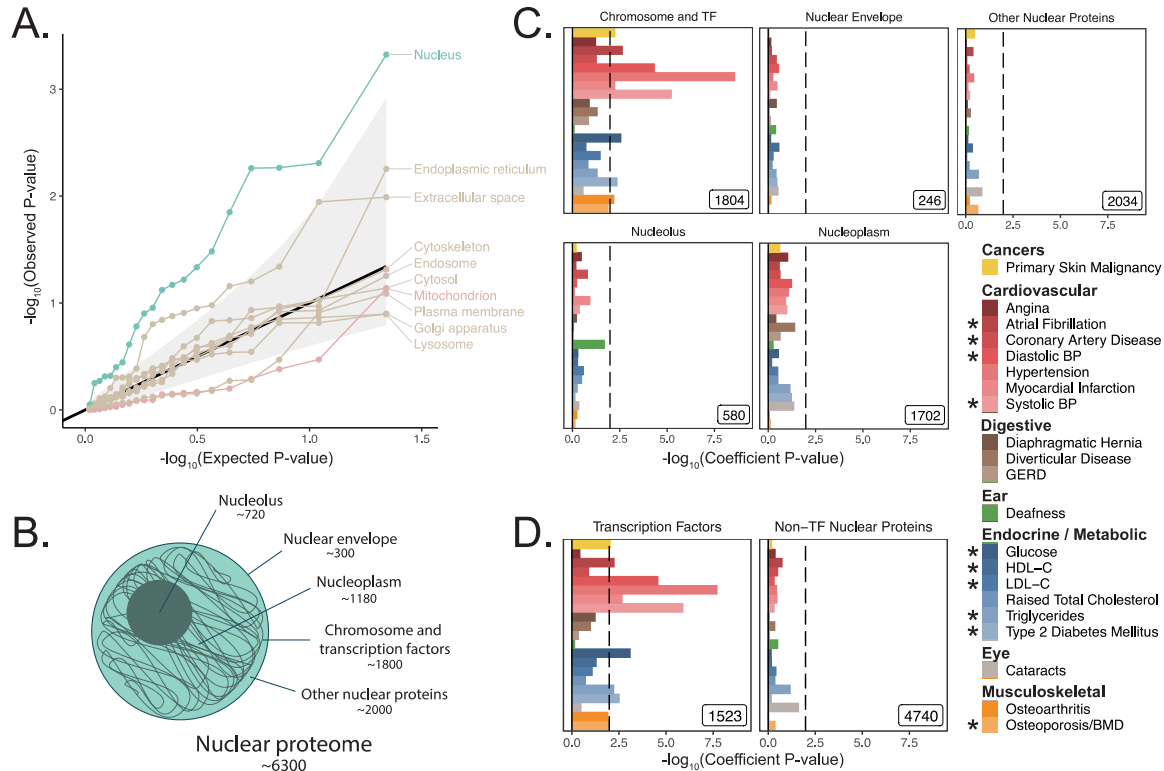


Figure 3. Heritability enrichment of organellar proteomes across age-related disease in UK Biobank. **A.** Quantile-quantile plot of heritability enrichment p-values atop the baseline model for gene-sets representing organellar proteomes, with black line representing expected null p-values following the uniform distribution and shaded ribbon representing 95% CI. **B.** Scheme of spatially distinct subsets of the nuclear proteome as a strategy to characterize observed enrichment of the nuclear proteome. Numbers represent gene-set size. **C.** S-LDSC enrichment p-values for spatial subsets of the nuclear proteome computed atop the baseline model. **D.** S-LDSC enrichment p-values for TFs and all other nucleus-localizing proteins. Inset numbers represent gene-set sizes, black lines represent cutoff at BH FDR < 10%. * represents traits for which sufficiently well powered cohorts from both UKB and meta-analyses were available.

172 We next asked whether heritability for age-related diseases and traits clusters among loci associated with
 173 any cellular organelle. We used the COMPARTMENTS database (<https://compartments.jensenlab.org>) to
 174 define gene-sets corresponding to the proteomes of nine additional organelles⁴⁶ besides mitochondria
 175 (**Methods**). We used S-LDSC to produce heritability estimates for these categories in the UKB age-related
 176 disease traits, finding evidence of heritability enrichment in many traits for genes comprising the nuclear
 177 proteome (**Figure 3A, Methods**). No other tested organelles showed evidence of heritability enrichment.
 178 Variation in or near genes comprising the nuclear proteome explained over 50% of disease heritability on
 179 average despite representing only ~35% of tested SNPs (**Figure 3-S1, Supplementary note**). We
 180 successfully replicated this pattern of heritability enrichment among organelles using MAGMA in UKB at
 181 two window sizes (**Figure 3-S3A, 3-S3B**), again finding enrichment only among genes related to the
 182 nucleus.

183

184 Much of the nuclear enrichment signal emanates from transcription factors

185

186 With over 6,000 genes comprising the nuclear proteome, we considered largely disjoint subsets of the
 187 organelle’s proteome to trace the source of the enrichment signal^{47–49} (**Figure 3B, Methods,**
 188 **Supplementary note**). We found significant heritability enrichment within the set of 1,804 genes whose
 189 protein products are annotated to localize to the chromosome itself ($q < 0.1$ for 9 traits, **Figure 3C, 3-S2A**).
 190 Further partitioning revealed that much of this signal is attributable to the subset classified as TFs⁴⁹ (1,523
 191 genes, $q < 0.1$ for 10 traits, **Figure 3D, 3-S2B**). We replicated these results using MAGMA in UKB at two
 192 window sizes (**Figure 3-S3**), and also replicated enrichments among TFs in several (but not all)
 193 corresponding meta-analyses (**Figure 3-S4**) despite reduced power (**Figure 2-S6H**). We generated
 194 functional subdivisions of the TFs (**Methods, Supplementary note**), finding that the non-zinc finger TFs
 195 showed enrichment for a highly similar set of traits to those enriched for the whole set of TFs (**Figure 3-**
 196 **S5D, 3-S6B, 3-S7B, 3-S8B**). Interestingly, the KRAB domain-containing zinc fingers (KRAB ZFs)⁵⁰, which are
 197 recently evolved (**Figure 3-S5H**), were largely devoid of enrichment even compared to non-KRAB ZFs
 198 (**Figure 3-S5E, 3-S6C, 3-S7C, 3-S8C**). Thus, we find that variation within or near non-KRAB domain-
 199 containing TF genes has an outside influence on age-associated disease heritability.

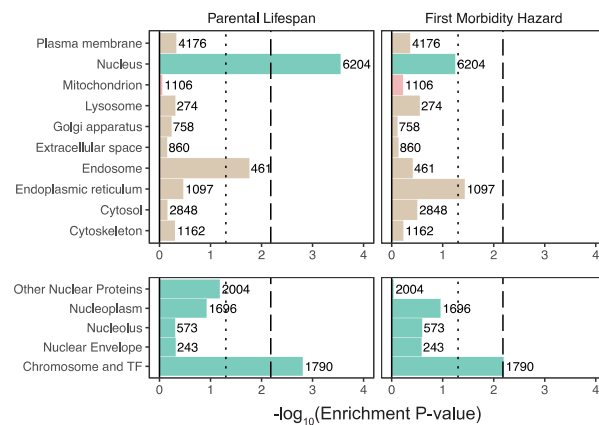


Figure 4. Enrichment of organellar proteomes within parental lifespan and healthspan as proxies for aging. Upper panels represent organelle proteomes; lower panels represent spatial subsets of the nuclear proteome. Numbers atop each bar represent gene-set sizes. Dashed lines represent cutoff at BH FDR < 10%, dotted lines represent nominal $p = 0.05$.

200 We next turned to recently published GWAS assessing parental lifespan⁵¹ and “healthspan” via first
 201 morbidity hazard⁵². Both traits showed highly significant heritability via S-LDSC ($h^2(s.e.) =$
 202 $0.0265 (0.0019)$ and $0.0348 (0.003)$ respectively, **Methods**). Enrichment analysis of organelles among
 203 these traits revealed a significant enrichment for the nucleus for parental lifespan ($p = 0.0003$) using
 204 MAGMA (**Figure 4, Table S7**). While we observed only a nominally “suggestive” enrichment for the nucleus
 205 for healthspan ($p = 0.058$), S-LDSC showed significant nuclear heritability enrichment ($p = 0.0016$, **Figure**
 206 **4-S1**). Analysis of spatial subsets of the nuclear proteome showed significant enrichment for TFs and
 207 proteins localizing to the chromosome in both aging phenotypes using MAGMA (**Figure 4**) and for
 208 healthspan using S-LDSC (**Figure 4-S1**).

209
 210

Mitochondrial genes tend to be more “haplosufficient” than genes encoding other organelles

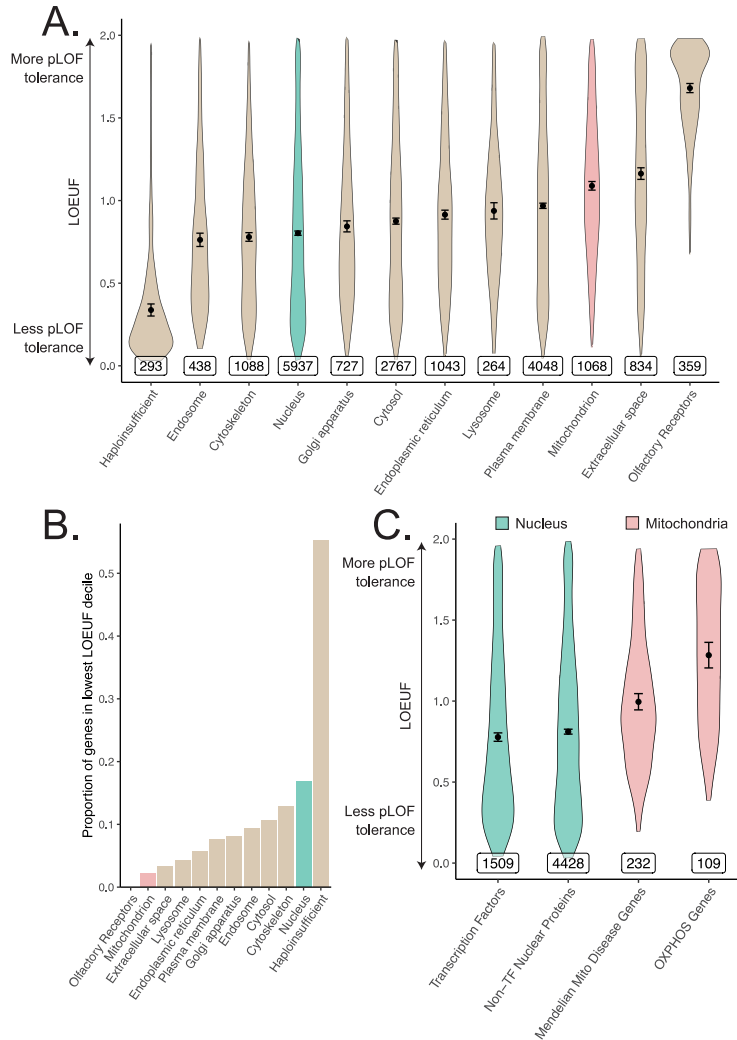


Figure 5. Differences in constraint distribution across organelles. **A.** Constraint as measured by LOEUF from gnomAD v2.1.1 for genes comprising organellar proteomes, book-ended by distributions for known haploinsufficient genes as well as olfactory receptors. Lower values indicate genes exacting a greater organismal fitness cost from a heterozygous LoF variant (greater constraint). **B.** Proportion of each gene-set found in the lowest LOEUF decile. Higher values indicate gene-sets containing more highly constrained genes. **C.** Constraint distributions for subsets of the nuclear-encoded mitochondrial proteome (red) and subsets of the nucleus (teal). Black points represent the mean with 95% CI. Inset numbers represent gene-set size.

211 In light of observing heritability enrichment only among nuclear transcription factors, we wanted to
 212 determine if the fitness cost of pLoF variation in genes across cellular organelles mirrored our results.
 213 Mitochondria-localizing genes and TFs play a central role in numerous Mendelian diseases^{23,53–55}, so we
 214 initially hypothesized that genes belonging to either category would be under significant purifying
 215 selection (i.e., constraint). We obtained constraint metrics from gnomAD
 216 (<https://gnomad.broadinstitute.org>)⁵⁶ as the LoF observed/expected fraction (LOEUF). In agreement with
 217 our GWAS enrichment results, we observed that the mitochondrion on average is one of the least
 218 constrained organelles we tested, in stark contrast to the nucleus (**Figure 5A**). In fact, the nucleus was
 219 second only to the set of “haploinsufficient” genes (defined based on curated human clinical genetic
 220 data⁵⁶, **Methods**) in the proportion of its genes in the most constrained decile, while the mitochondrion
 221 lay on the opposite end of the spectrum (**Figure 5B**). Interestingly, even the Mendelian mitochondrial
 222 disease genes had a high tolerance to pLoF variation on average in comparison to TFs (**Figure 5C**). Even
 223 across different categories of TFs, we observed that highly constrained TF subsets tend to show GWAS

224 enrichment (**Figure 5-S1, 3-S5E**) relative to unconstrained subsets for our tested traits. Indeed, explicit
225 inclusion of LOEUF as a covariate in the enrichment analysis model (**Methods**) reduced the significance of
226 (but did not eliminate) the enrichment seen for the TFs (**Figure 5-S2B, 5-S3B, 5-S2E, 5-S2F**). Thus, while
227 disruption in both mitochondrial genes and TFs can produce rare disease, the fitness cost of heterozygous
228 variation in mitochondrial genes appears to be far lower than that among TFs. This dichotomy reflects the
229 contrasting enrichment results between mitochondrial genes and TFs and supports the importance of
230 gene regulation as it relates to evolutionary conservation.

231

232 **Discussion**

233 Pathology in cellular organelles has been widely documented in age-related diseases^{3,7,57-60}. Using a
234 human genetics approach, here we report the unexpected discovery that except for the nucleus, cellular
235 organelles tend not to be enriched in genetic associations for common, age-related diseases. We started
236 with a focus on the mitochondria as a decline in mitochondrial abundance and activity has long been
237 reported as one of the most consistent correlates of aging^{14,16,18,22} and age-associated diseases^{10-13,15,17,19-}
238 ²¹. We tested common variants contributing to the mitochondrial proteome on the nucDNA and mtDNA
239 and found no convincing evidence of heritability enrichment in any tested trait, cohort, or method. We
240 systematically expanded our analysis to survey 10 organelles and found that only the nucleus showed
241 enrichment, with much of this signal originating from nuclear TFs. Constraint analysis showed a substantial
242 fitness cost to heterozygous loss-of-function mutation in genes encoding the nuclear proteome, whereas
243 genes encoding the mitochondrial proteome were “haplosufficient.”

244 Here, we focus on enrichment to place the complex genetic architectures of age-related traits in a broader
245 biological context and prioritize pathways for follow-up. For these highly polygenic traits, any large
246 fraction of the genome may explain a statistically significant amount of disease heritability^{61,62}, and indeed
247 associations between individual organelle-relevant loci and certain common diseases have been identified
248 previously^{63,64}. For example, variants in the endoplasmic reticular genes *WFS1* and *ATF6B* and the
249 mitochondrial gene *ATP5G1* have been associated with common T2D⁶⁵. These genes are present in the
250 respective organelle gene-sets, however unlike TFs, neither the endoplasmic reticulum nor the
251 mitochondrion showed enrichment for T2D. Importantly, both MAGMA and S-LDSC are capable of
252 detecting an enrichment even in a highly polygenic background. Both methods have been used in the past
253 to identify biologically plausible disease-relevant tissues^{38,43} and pathway enrichments^{66,67} in traits across
254 the spectrum of polygenicity, and we identify enrichments among disease-relevant tissues using both
255 methods in several highly polygenic traits.

256 While previous work has shown that common disease GWAS can be enriched for expression in specific
257 disease-relevant organs^{43,68}, our data suggest that this framework does not generally extend from organs
258 to organelles. This finding contrasts with our classical nosology of inborn errors of metabolism that tend
259 to be mapped to “causal” organelles, e.g., lysosomal storage diseases, disorders of peroxisomal
260 biogenesis, and mitochondrial OXPHOS disorders. The observed enrichment for TFs within the nucleus
261 indicates that common variation influencing genome regulation impacts common disease risk more than
262 variation influencing individual organelles.

263 Our analysis of common inherited mitochondrial variation represents, to our knowledge, the most
264 comprehensive joint assessment of mitochondria-relevant nucDNA and mtDNA variation in age-related
265 diseases. We replicated mtDNA associations with creatinine and AST observed previously in BioBank
266 Japan⁴⁵, further supporting our approach. While individual mtDNA variants have been previously
267 associated with certain traits⁶⁹⁻⁷¹, these associations appear to be conflicting in the literature, perhaps
268 because of limited power and/or uncontrolled confounding biases such as population stratification^{72,73}.
269 Our negative results are surprising, but they are compatible with a prior enrichment analysis focused on

270 T2D⁷⁴ as well as a small number of isolated reports interrogating either mitochondria-relevant nucDNA⁷⁴
271 or mtDNA^{45,75-77} loci in select diseases.

272 To our knowledge, we are the first to systematically document heterogeneity in average pLoF across
273 cellular organelles. That MitoCarta genes are “haplosufficient” and pLoF tolerant (**Figure 5A**) is consistent
274 with the observation that most of the ~300 inborn mitochondrial disease genes produce disease with
275 recessive inheritance²³ and healthy parents. The few mitochondrial disorders that show autosomal
276 dominant inheritance are nearly always due to dominant negativity rather than haploinsufficiency. The
277 intolerance of TFs to pLoF variation (**Figure 5C**) provide a stark contrast to the results from the
278 mitochondria that is borne out in their associated Mendelian disease syndromes: TFs are known to be
279 haploinsufficient⁷⁸ and even regulatory variants modulating their expression can produce severe
280 Mendelian disease⁷⁹. We observe enrichment among TFs for 10 different diseases as well as parental
281 lifespan and healthspan, consistent with observed elevated purifying selection against pLoF variants in
282 these genes. Our enrichment results combined with pLoF intolerance suggest that variation among TFs
283 may produce disease-associated variants with larger effect sizes than expectation, underscoring their
284 importance as genetic “levers” for common disease heritability.

285 Why are mitochondria so robust to variation in gene dosage (**Figure 5**) and hence “haplosufficient?” We
286 propose two possibilities. First, mitochondrial pathways tend to be highly interconnected, and it was
287 already proposed by Wright⁸⁰ and later by Kacser and Burns⁸¹ that haplosufficiency arises as a
288 consequence of physiology, i.e., system output is inherently buffered against the partial loss of a single
289 gene due to the network organization of metabolic reactions. Kacser and Burns in fact explicitly mention
290 that noncatalytic gene products fall outside their framework, and we believe that our finding that nucleus-
291 localizing and cytoskeletal genes are the two most pLoF-intolerant compartments is consistent with their
292 assessment. Second, mitochondria were formerly autonomous microbes and hence may have retained
293 vestigial layers of “intra-organelle buffering” against genetic variation. Numerous feedback control
294 mechanisms, including respiratory control⁸², help to ensure organelle robustness across physiological
295 extremes^{83,84}. In fact, a recent CRISPR screen showed that of the genes for which knock-out modified
296 survival under a mitochondrial poison, there is a striking over-representation of genes that themselves
297 encode mitochondrial proteins⁸⁵.

298 Throughout this study, we have tested for enrichment among inherited common variant associations near
299 genes via an additive genetic model. We acknowledge the limitations of focusing on a specific genetic
300 model and variant frequency regime, though note that common variation is the largest documented
301 source of narrow-sense heritability, which typically accounts for a majority of disease heritability^{86,87}. First,
302 we consider only common variants. While rare variants may prove to be instructive, it is notable that a
303 previous rare variant analysis in T2D⁸⁸ failed to show enrichment among OXPHOS genes. Second, we
304 consider only additive genetic models. A recessive model may be particularly fruitful for mitochondrial
305 genes given their tolerance to pLoF variation, however these models are frequently power-limited and
306 may not explain much more phenotypic variance than additive models^{89,90}. Third, we have not considered
307 epistasis. The effects of mtDNA-nucDNA interactions⁹¹ in common diseases have yet to be assessed. While
308 there is debate about whether biologically-relevant epistasis can be simply captured by main
309 effects^{87,89,92,93} at individual loci, it is possible that modeling mtDNA-nucDNA interactions will reveal new
310 contributions. Fourth, to systematically assess all organelles, we restrict our analyses to variants near
311 genes comprising each organelle’s proteome. It remains possible that future work will systematically
312 identify novel organelle-relevant loci elsewhere in the genome which contribute disproportionately to
313 age-related trait heritability. Fifth, while we are well-powered to detect physiologically relevant
314 enrichments among most tested organelles (including the mitochondrion), our power may be more
315 limited for particularly small compartments (e.g., lysosome). Finally, it is crucial not to confuse our mtDNA-

316 GWAS results with previously reported associations between somatic mtDNA mutations and age-
317 associated disease^{13,14,22} – the present work is focused on germline variation.

318 We have not formally addressed the causality of mitochondrial dysfunction in common age-related
319 disease and the observed lack of heritability enrichment does not preclude the possibility of a therapeutic
320 benefit in targeting the mitochondrion for age-related disease. For example, mitochondrial dysfunction is
321 documented in brain or heart infarcts following blood vessel occlusion in laboratory-based models^{94,95}.
322 Clearly mitochondrial genetic variants do not influence infarct risk in this laboratory model, but
323 pharmacological blockade of the mitochondrial permeability transition pore can mitigate reperfusion
324 injury and infarct size⁹⁶. Future studies will be required to determine if and how the mitochondrial
325 dysfunction associated with common age-associated diseases can be targeted for therapeutic benefit.
326 Efforts to develop reliable measures of mitochondrial function and dysfunction have the potential to
327 unbiasedly discover genetic instruments that influence the mitochondrion, and causal inference
328 techniques such as Mendelian Randomization may shed light on this important causal question.

329 Our finding that the nucleus is the only organelle that shows enrichment for common age-associated trait
330 heritability builds on prior work implicating nuclear processes in aging. Most human progeroid syndromes
331 result from monogenic defects in nuclear components⁹⁷ (e.g., *LMNA* in Hutchinson-Gilford progeria
332 syndrome, *TERC* in dyskeratosis congenita), and telomere length has long been observed as a marker of
333 aging⁹⁸. Heritability enrichment of age-related traits among gene regulators is consistent with the
334 epigenetic dysregulation⁹⁹ and elevated transcriptional noise^{3,100} observed in aging (e.g., *SIRT6* modulation
335 influences mouse longevity¹⁰¹ and metabolic syndrome⁵⁸). An important role for gene regulation in
336 common age-related disease is in agreement with both the observation that a very large fraction of
337 common disease-associated loci corresponds to the non-coding genome and the enrichment of disease
338 heritability in histone marks and TF binding sites^{38,102}. Given that a deterioration in several other cellular
339 organelles has been so frequently documented in age-related traits, a future challenge lies in elucidating
340 how inherited variation in or near TFs ultimately leads to the observed organelle dysfunction in age-
341 related disease.

342

343 **Acknowledgements**

344 We thank D. Altshuler, S.E. Calvo, T. Finkel, H. Finucane, E.S. Lander, M.E. MacDonald, D. Palmer, E.B.
345 Robinson, A.V. Segrè, M.E. Talkowski, R.K. Walters, C.C. Winter, and members of the Mootha and Neale
346 labs for critical feedback and discussions. This research has been conducted using the UK Biobank
347 Resource under Application Number 31063. This project was supported in part by grants (NIH
348 R35GM122455 to V.K.M. and NIH T32 AG000222 to R.G.) from the National Institutes of Health. VKM is
349 an Investigator of the Howard Hughes Medical Institute.

350

351 **Data Availability**

352 Heritability point estimates and standard errors for age-related traits are listed in Table S1. Genetic and
353 phenotypic correlation point estimates and standard errors/p-values plotted in Figure 1B are available in
354 Table S2. Summary statistics from mtDNA-GWAS are available in Table S4. All gene-based enrichment
355 analysis p-values and point estimates are available in Tables S6 and S7. Period prevalence data for diseases
356 in the UK can be obtained from Kuan et al. 2019. Gene-sets can be found using COMPARTMENTS
357 (<https://compartments.jensenlab.org>), MitoCarta 2.0
358 (<https://www.broadinstitute.org/files/shared/metabolism/mitocarta/human.mitocarta2.0.html>),
359 Lambert et al. 2018 (DOI: 10.1016/j.cell.2018.01.029), Frazier et al. 2019 (DOI: 10.1074/jbc.R117.809194),
360 Finucane et al. 2018 (<https://alkesgroup.broadinstitute.org/LDSCORE/>), Kapopoulou et al. 2015 (DOI:
361 10.1111/evo.12819), and the Macarthur laboratory (https://github.com/macarthur-lab/gene_lists). Gene

362 age estimates were obtained from Litman, Stein 2019 (DOI: 10.1053/j.seminoncol.2018.11.002). GWAS
363 catalog annotations can be obtained from: <https://www.ebi.ac.uk/gwas>. Heritability estimates across UKB
364 can be obtained at: https://nealelab.github.io/UKBB_ldsc/. UKB summary statistics can be obtained from
365 Neale lab GWAS round 2: https://github.com/Nealelab/UK_Biobank_GWAS. Annotations for the Baseline
366 v1.1 and BaselineLD v2.2 models as well as other relevant reference data, including the 1000G EUR
367 reference panel, can be obtained from <https://alkesgroup.broadinstitute.org/LDSCORE/>. eQTL and
368 expression data in human tissues can be obtained from GTEx (<https://www.gtexportal.org>). Constraint
369 estimates can be found via gnomAD: <https://gnomad.broadinstitute.org>. See citations for publicly
370 available GWAS meta-analysis summary statistics^{28–37,51,52}.

371

372 **Code Availability**

373 Our analysis leverages publicly available tools including LDSC for heritability enrichment and genetic
374 correlation (<https://github.com/bulik/ldsc>), MAGMA v1.07b for gene-set enrichment analysis
375 (<https://ctg.cncr.nl/software/magma>), and Hail v0.2.51 for distributed computing and mtDNA GWAS
376 (<https://hail.is>).

377

378 **Competing Interests**

379 VKM is an advisor to and receives compensation or equity from Janssen Pharmaceuticals, 5am Ventures,
380 and Raze Therapeutics. BMN is a member of the scientific advisory board at Deep Genomics and RBNC
381 Therapeutics. BMN is a consultant for Camp4 Therapeutics, Takeda Pharmaceutical and Biogen. KJK is a
382 consultant for Vor Biopharma.

383

384 **Author Contributions**

385 R.G., B.M.N., and V.K.M. conceived of the project; R.G., K.J.K., D.H. designed analyses; R.G. performed
386 analyses; B.M.N., V.K.M. supervised project; R.G. and V.K.M. wrote the manuscript with input from
387 other authors.

388 **Materials and Methods**

389 Trait selection:

390 Sex-standardized period prevalence of over 300 diseases was obtained from an extensive survey of the
391 National Health Service in the UK as reported previously²⁶. To select high prevalence late-onset diseases,
392 we ranked diseases with a median onset over 50 years of age by the sum of the period prevalence of all
393 age categories above 50. We selected the top 30 diseases using this metric and manually mapped these
394 traits to similar or equivalent phenotypes with publicly available summary statistics from UKB and/or well-
395 powered meta-analyses (e.g., Parkinson's Disease and Alzheimer's Disease for dementia) resulting in 24
396 traits with data available in UKB, meta-analyses, or both (**Table S1**).

397

398 Criteria for inclusion of summary statistics:

399 We manually mapped selected age-related diseases and traits to corresponding phenotypes in UKB. In
400 parallel, we searched the literature to identify well-powered EUR-predominant GWAS (referred to as
401 meta-analyses) that (1) used primarily non-targeted arrays, (2) had publicly available full summary
402 statistics, and (3) did not enroll individuals from UKB to serve as independent replication (**Supplementary**
403 **note**). We produced heritability estimates using stratified linkage-disequilibrium score regression (S-LDSC,
404 <https://github.com/bulik/ldsc>)³⁸ atop the BaselineLD v2.2 model using reference LD scores computed
405 from 1000G EUR (<https://alkesgroup.broadinstitute.org/LDSCORE/>). We computed the heritability Z-
406 score, a statistic that captures sample size, polygenicity, and heritability³⁸, and included only traits with
407 heritability Z-score > 4 (**Supplementary note**) for further analysis.

408

409 Genetic correlations among age-related traits:

410 Pairwise genetic correlations, r_g , were computed using linkage-disequilibrium score correlation³⁹ on all
411 selected age-related traits with heritability Z-score > 4. We used UKB summary statistics
412 (https://github.com/Nealelab/UK_Biobank_GWAS) for all sufficiently powered traits; summary statistics
413 from meta-analyses were used for eGFR³⁵, Alzheimer's Disease³⁷, and Parkinson's Disease³⁶ as these traits
414 showed heritability Z-score > 4 within meta-analyses but not in UKB (**Table S1**). P-values for genetic
415 correlation represented deviation from the null hypothesis $r_g = 0$. Traits were ordered by their
416 contribution to the first eigenvector of the absolute value of the correlation matrix, with point estimates
417 and standard errors available in **Table S2**. Bonferroni correction was applied producing a p-value cutoff of
418 $0.05 / \left[\binom{24}{2} + \binom{21}{2} \right] = 1.03 * 10^{-4}$, accounting for both genotypic and phenotypic correlation hypothesis
419 tests.

420

421 Phenotypic correlations in UKB:

422 Pairwise phenotypic correlations, r_p , were computed for all 21 traits with well-powered individual level
423 data available in UKB (**Table S1**). Pearson correlation was computed between continuous traits via
424 `cor.test` in R with a two-sided alternative. Tetrachoric correlation was used to compute correlations
425 between binary traits and biserial correlation was used for correlations between binary and continuous
426 traits, using the `polychor` and `polyserial` functions of the `polycor` package in R respectively using
427 the two-step approximation. These approaches model a latent normally distributed variable underlying
428 binary traits. P-values were computed using a normal approximation using standard error estimates from
429 `polycor`. Point estimates and standard errors are available in **Table S2**.

430

431 Assessment of mitochondria-localizing genes in the GWAS Catalog:

432 We mapped variants in the GWAS Catalog (obtained on September 5th, 2019,
433 <https://www.ebi.ac.uk/gwas/>) meeting genome-wide significance ($p < 5e-8$) to genes using provided
434 annotations, producing a set of trait-associated genes for each trait. We manually selected phenotypes

435 represented in the GWAS Catalog matching our set of age-associated traits with > 30 trait-associated
436 genes. For each trait, we computed the proportion of trait-associated genes that were mitochondria-
437 localizing (defined via MitoCarta2.0⁴¹) and tested for enrichment or depletion relative to overall genome
438 background using two-sided Fisher's exact tests correcting for multiple hypothesis tests with the
439 Benjamini-Hochberg (BH) procedure at FDR q-value < 0.1.

440 We also computed the test statistic N_g^{enrich} , defined as the number of age-associated traits showing a
441 nominal (not necessarily statistically significant) enrichment for a given gene-set g , for the MitoCarta
442 genes. We then generated an empirical null distribution for N_g^{enrich} . We drew 1,000 random samples of
443 protein-coding genes, where each sample contained the same number of genes as the set of
444 mitochondria-localizing genes and computed N_g^{enrich} for each of these gene-sets (**Figure 2-S1B**). The one-
445 sided p-value, defined as $\Pr(N_g^{enrich} \leq x)$ under the null, was subsequently obtained.

446 We expanded our enrichment/depletion analysis to all 332 traits in the GWAS Catalog with over 30 trait-
447 associated genes; for enrichment or depletion testing, we used two-sided Fisher's exact tests and
448 corrected for multiple hypothesis testing with the BH procedure at FDR q-value < 0.1.

449
450 Harmonization and filtering of summary statistics for LDSC and MAGMA:
451 UKB summary statistics previously formatted for use with LDSC and filtered to HapMap3 (HM3) SNPs
452 (https://github.com/Nealelab/UKBB_Idsc) were used for analysis with S-LDSC. For analysis with MAGMA
453 v1.07b⁴⁴, we included variants from the full Neale Lab UKB Round 2 GWAS summary statistics
454 (https://github.com/Nealelab/UK_Biobank_GWAS) with INFO > 0.8 and MAF > 0.01, and excluded any
455 variants flagged as low confidence (a heuristic defined by MAF < 0.001 or expected case MAC < 25).

456 Summary statistics obtained from publicly available GWAS meta-analyses²⁸⁻³⁷ were reported in varied
457 formats. We manually verified the genome build upon which each meta-analysis reported results and
458 ensured that all sets of summary statistics contained columns listing P-value, variant rsID, genome-build
459 specific coordinates, and if available, variant-specific sample size (**Table S1**). If variant coordinates or rsID
460 were not provided, the relevant columns were obtained from dbSNP database version 130 (for hg18) or
461 146 (for hg19). We used the summary statistic munging script provided with S-LDSC
462 (<https://github.com/bulik/ldsc>) to generate summary statistics compatible with S-LDSC, restricting to
463 HM3 SNPs as these tend to be best behaved for analysis with LDSC. For use of meta-analyses with
464 MAGMA⁴⁴, we restricted analysis to variants with INFO > 0.8 and MAF > 0.01 if such information was
465 provided.

466
467 Multiple testing correction for gene-set enrichment analysis:
468 To account for the multiple hypothesis tests performed throughout this study for age-related traits, we
469 obtained p-value thresholds via the BH procedure at FDR < 0.1 for all gene-sets assessed for a given
470 method and cohort type (where the two cohort types were UKB and meta-analysis). The BH procedure at
471 FDR < 0.1 was also applied to our analyses of parental lifespan and healthspan.

472
473 Gene-set based enrichment analysis:
474 We extensively use S-LDSC and MAGMA to perform gene-set enrichment analyses among GWAS summary
475 statistics. To test enrichment with S-LDSC, SNPs were mapped to each gene with a 100kb symmetric
476 window as recommended⁴³ and LD scores were computed using the 1000G EUR reference panel
477 (<https://alkesgroup.broadinstitute.org/LDSCORE/>) and subsequently restricted to the HM3 SNPs. We
478 used S-LDSC to test for heritability enrichment controlling for 53 annotations including coding regions,
479 enhancer regions, 5' and 3' UTRs, and others as previously described³⁸ (baseline v1.1, referred to as
480 baseline model hereafter). We also used MAGMA with both 5kb up, 1.5kb down and 100kb symmetric

481 windows to test for enrichment. MAGMA gene-level analysis was performed with the 1000G EUR LD
482 reference panel to account for LD structure, and gene-set analysis was performed including covariates for
483 gene length, variant density, inverse minor allele count (MAC), as well as log-transformed versions of
484 these covariates. Statistical tests for both S-LDSC and MAGMA were one-sided, considering enrichment
485 only. For both methods, we included the relevant superset of genes as a control to ensure that our analysis
486 was competitive (**Supplementary note**). We refer to this approach as the ‘usual approach’. All enrichment
487 effect size estimates and p-values are available in **Tables S6** and **Table S7**.

488

489 Enrichment analysis of genes comprising the mitochondrial proteome:

490 We obtained the set of nuclear-encoded mitochondria-localizing genes using MitoCarta2.0⁴¹ and used the
491 literature to obtain the subset of MitoCarta genes involved in inherited mitochondrial disease²³ as well as
492 those producing components of oxidative phosphorylation (OXPHOS) complexes. We used both S-LDSC
493 and MAGMA to test for enrichment in the usual way (**Methods**) controlling for the set of protein-coding
494 genes to ensure a competitive analysis (**Supplementary note**). We also tested mitochondria-localizing
495 genes for enrichment in meta-analyses using S-LDSC and MAGMA with the same parameters as for UKB
496 traits (**Supplementary note**).

497

498 Tissue-expressed gene-set enrichment analysis:

499 To obtain the set of genes most expressed in a given tissue versus others, we obtained t-statistics
500 computed from GTEx v6 gene-level transcript-per-million (TPM) data corrected for age and sex as
501 published previously⁴³. For each tissue, we selected the top 2485 genes (10%) with the highest t-statistics
502 for tissue-specific expression, producing tissue-expressed gene-sets. We selected nine tissues based on
503 expectation of enrichment for our tested traits in UKB (e.g., liver for LDL levels, esophageal mucosa for
504 GERD). We used both S-LDSC and MAGMA to test for enrichment in the usual way (**Methods**) controlling
505 for the set of tissue-expressed genes to ensure a competitive analysis (**Supplementary note**). Tissue-
506 expressed gene-set analyses were performed on meta-analyses with S-LDSC and MAGMA on the same
507 tissues using the same parameters as used in UKB.

508

509 Power analysis:

510 To test for the effects of gene-set size on power, we selected ten positive control tissue-trait pairs based
511 on (1) the presence of tissue enrichment in UKB with S-LDSC and MAGMA and (2) if the observed
512 enrichment was biologically plausible. The pairs tested were liver-HDL, liver-LDL, liver-TG, liver-
513 cholesterol, pancreas-glucose, pancreas-T2D, atrial appendage-atrial fibrillation, sigmoid colon-
514 diverticular disease, coronary artery-myocardial infarction, and visceral adipose-HDL. We then, in brief,
515 used an empirical sampling-based approach, generating random subsamples of a selected set of tissue-
516 expressed gene-sets at four different gene-set sizes (1523, 1105, 800, and 350 genes), defining power as
517 the proportion of trials showing a significant enrichment (**Supplementary note**). We used the same sub-
518 sampled gene-sets for enrichment analysis using both S-LDSC and MAGMA in the usual way (**Methods**)
519 controlling for the set of tissue-expressed genes to ensure a competitive analysis (**Supplementary note**).
520 We used the same gene-sets among the subset of the positive control traits that showed enrichment in
521 the corresponding meta-analysis to verify power for the meta-analyses (**Supplementary note**).

522

523 Cross-tissue eQTL analysis

524 We obtained the set of eGenes from GTEx v8 across 49 tissues (<https://www.gtexportal.org>), filtering to
525 only include cis-eQTLs with q-value < 0.05. To determine how the landscape of cis-eQTLs for MitoCarta
526 genes compared to other protein-coding genes, we regressed the number of tissues with a detected cis-
527 eQTL for a given gene x , N_x^{eQTL} , onto an indicator for membership in a given organellar proteome

528 ($I_x^{organelle}$), controlling for gene length, log gene length, breadth of expression (τ_x), and the number of
529 tissues with detected expression > 5 TPM ($N_x^{express}$, **Supplementary note**). To quantify breadth of
530 expression, we obtained median-per-tissue GTEx v8 TPM expression values and computed τ^{103} after
531 removing lowly-expressed genes with maximal cross-tissue TPM < 1, defined as:

532

$$533 \quad \tau_x = \frac{\sum_{i=1}^n (1 - \hat{x}_i)}{n - 1} \text{ where } \hat{x}_i = \frac{x_i}{\max_{1 \leq i \leq n} x_i}$$

534

535 where x_i is the expression of gene x in tissue i with n tissues. τ ranges from 0 to 1, with lower τ indicating
536 broadly expressed gene and higher τ indicating more tissue specific expression patterns. Because GTEx
537 sampled multiple tissue subtypes (e.g., brain sub-regions) that show correlated expression profiles¹⁰⁴
538 which bias τ_x , N_x^{eQTL} , and $N_x^{express}$ upward, for each broader tissue class (brain, heart, artery, esophagus,
539 skin, cervix, colon, adipose) we selected a single representative tissue when computing these quantities
540 (**Figure 3-S5B, Supplementary note**). We used LD scores computed from the 1000G EUR reference panel.
541 The model, fit via OLS for each tested organelle, was:

542

$$543 \quad N_x^{eQTL} \sim I_x^{organelle} + N_x^{express} + \tau_x + \log(\text{gene length}) + \text{gene length}$$

544

545 mtDNA-wide association study:

546 We obtained mtDNA genotype data on 265 variants as obtained on the UK Biobank Axiom array and the
547 UK BiLEVE array from the full UKB release²⁷. To perform variant QC, we used evoker-lite¹⁰⁵ to generate
548 fluorescence cluster plots per-variant and per-batch and manually inspected the results, removing 19
549 variants due to cluster plot abnormalities (**Table S3, Supplementary note**). We additionally removed any
550 variants with heterozygous calls, within-array-type call rate < 0.95, and with less than 20 individuals with
551 an alternate genotype. For case-control traits, we removed any phenotype-variant pair with an expected
552 case count of alternate genotype individuals of less than 20, resulting in a maximum of 213 variants tested
553 per trait (**Supplementary note**). To perform sample QC, we restricted samples to the same samples from
554 which UKB summary statistics were generated (https://github.com/Nealelab/UK_Biobank_GWAS),
555 namely unrelated individuals 7 standard deviations away from the first 6 European sample selection PCs
556 with self-reported white-British, Irish, or White ethnicity and no evidence of sex chromosome aneuploidy.
557 We additionally removed any samples with within-array-type mitochondrial variant call rate < 0.95,
558 resulting in 360,662 unrelated samples of EUR ancestry. We generated the LD matrix for mitochondrial
559 DNA variants using Hail v0.2.51 (<https://hail.is>) pairwise for all 213 variants tested across all post-QC
560 samples.

561 We ran mtDNA-GWAS for all 21 UKB age-related phenotypes as well as creatinine and AST using Hail
562 v0.2.51 via linear regression controlling for the first 20 PCs of the nuclear genotype matrix, sex, age, age²,
563 sex*age, and sex*age² as performed for the UKB GWAS
564 (https://github.com/Nealelab/UK_Biobank_GWAS). We also used Hail to run Firth logistic regression with
565 the same covariates for case/control traits. As we observed that some mitochondrial DNA variants were
566 specific to array type, we also ran linear regression including array type as a covariate; we did not perform
567 logistic regression with array type as a covariate due to convergence issues from complete separation of
568 variants assessed only on a single array type. We defined mtDNA-wide significance using a Bonferroni
569 correction by $p = \frac{0.05}{4337} \approx 1.15e - 5$.

570

571 Enrichment analysis of components of organellar proteomes:

572 COMPARTMENTS (<https://compartments.jensenlab.org>)⁴⁶ is a resource integrating several lines of
573 evidence for protein localization predictions including annotations, text-mining, sequence predictions,
574 and experimental data from the Human Protein Atlas. We used this resource to obtain the degree of
575 evidence (a number ranging from 0 to 5) linking each gene to localization to one of 12 organelles: nucleus,
576 cytosol, cytoskeleton, peroxisome, lysosome, endoplasmic reticulum, Golgi apparatus, plasma
577 membrane, endosome, extracellular space, mitochondrion, and proteasome. To avoid noisy localization
578 assignments due to weak text mining and prediction evidence, we only considered localization
579 assignments with a score > 2 as described previously⁴⁶. We subsequently assigned compartment(s) to each
580 gene by selecting the compartment(s) with the maximal score within each gene. We only included
581 compartments containing over 240 genes due to limited power at smaller gene-set sizes and used
582 MitoCarta2.0⁴¹ to obtain a higher confidence set of genes localizing to the mitochondrion, resulting in
583 gene-sets representing the proteomes of 10 organelles. S-LDSC and MAGMA were used to test for
584 enrichment across the UKB age-related traits for these gene-sets in the usual way, controlling for the set
585 of protein-coding genes. S-LDSC was also used to obtain estimates of the percentage of heritability
586 explained by each organelle gene-set.

587

588 Enrichment analysis of spatial components of the nucleus:

589 To produce interpretable sub-divisions of the nucleus, we used Gene Ontology (GO)^{47,48} to identify terms
590 listed as children of the nucleus cellular component (GO:0005634). We used Ensembl version 99¹⁰⁶ to
591 obtain a first pass set of genes annotated to each sub-compartment of the nucleus (or its children). After
592 manual review of sub-compartments with > 90 genes, we selected nucleoplasm (GO:0005654), nuclear
593 chromosome (GO:0000228), nucleolus (GO:0005730), nuclear envelope (GO:0005635), splicosomal
594 complex (GO:0005681), nuclear DNA-directed RNA polymerase complex (GO:0055029), and nuclear pore
595 (GO:0005643). We excluded terms listed as 'part' due to poor interpretability and manually excluded
596 similar terms (e.g., nuclear lumen vs nucleoplasm). To generate a high confidence set of genes localizing
597 to each of these selected sub-compartments, we then turned to the COMPARTMENTS resource which
598 assigns localization confidence scores for each protein to GO cellular component terms. We assigned
599 members of the nuclear proteome to these selected nuclear sub-compartments using same the approach
600 outlined for the organelle analysis (**Methods**). After filtering our selected sub-compartments to those
601 containing > 240 genes, we obtained four categories: nucleoplasm, nuclear chromosome, nucleolus, and
602 nuclear envelope. The nuclear chromosome annotation was largely overlapping with a manually curated
603 high-quality list of TFs⁴⁹ however was not exhaustive; as such, we merged these lists to generate the
604 chromosome and TF category. To improve interpretability, we removed genes from nucleoplasm that
605 were also assigned to another nuclear sub-compartment, constructed a list of other nucleus-localizing
606 proteins not captured in these four sub-compartments, and included only genes annotated as localizing
607 to the nucleus (**Methods**). S-LDSC and MAGMA were used to test for enrichment across the UKB age-
608 related traits for these gene-sets in the usual way while controlling for the set of protein-coding genes
609 (**Methods**).

610

611 Enrichment analysis of functionally distinct TF subsets:

612 We used a published curated high-quality list of TFs⁴⁹ to partition the Chromosome and TF category into
613 TFs and other chromosomal proteins. To determine which TFs are broadly expressed versus tissue specific,
614 we computed τ per TF across all selected tissues after removing lowly-expressed genes with maximal
615 cross-tissue TPM < 1 (**Methods, Supplementary note**). The threshold for tissue-specific genes was set at
616 $\tau \geq 0.76$ based on the location of the central nadir of the resultant bimodal distribution (**Figure 3-S5A**).
617 To identify terciles of TFs by age, we obtained relative gene age assignments for each gene previously
618 generated by obtaining the modal earliest ortholog level across several databases mapped to 19 ordered
619 phylostrata¹⁰⁷. DNA binding domain (DBD) annotations for the TFs were obtained from previous manual

620 curation efforts⁴⁹. S-LDSC and MAGMA were used to test for enrichment across the UKB age-related traits
621 for these gene-sets in the usual way while controlling for the set of protein-coding genes (**Methods**). We
622 also tested TFs for enrichment in meta-analyses using S-LDSC and MAGMA with the same parameters as
623 for UKB traits (**Supplementary note**).

624

625 *Analysis of constraint across organelles and sub-organelle gene-sets:*

626 We obtained gene-level gnomAD v2.1.1 constraint tables (<https://gnomad.broadinstitute.org>),
627 haploinsufficient genes, and olfactory receptors⁵⁶ (https://github.com/macarthur-lab/gene_lists).
628 Constraint values as loss-of-function observed/expected fraction (LOEUF) were mapped to genes within
629 organelle, sub-mitochondrial, sub-nuclear, and TF binding domain gene-sets.

630

631 *Enrichment analysis across age-related disease holding constraint as a covariate:*

632 To test for enrichment with constraint as a covariate, we used MAGMA with UKB age-related traits. We
633 mapped variants to genes and performed the gene-level analysis as done previously for the mitochondria-
634 localizing gene and organelle analysis. We included LOEUF and log LOEUF as covariates for the gene-set
635 analysis in addition to the default covariates (gene length, SNP density, inverse MAC, as well as the
636 respective log-transformed versions) via the `-condition-residualize` flag.

- 637 1. Wang K, Gaitsch H, Poon H, Cox NJ, Rzhetsky A. Classification of common human diseases derived
638 from shared genetic and environmental determinants. *Nat Genet.* 2017;49(9):1319-1325.
639 doi:10.1038/ng.3931
- 640 2. Claussnitzer M, Cho JH, Collins R, et al. A brief history of human disease genetics. *Nature.*
641 2020;577(7789):179-189. doi:10.1038/s41586-019-1879-7
- 642 3. López-Otín C, Blasco MA, Partridge L, Serrano M, Kroemer G. The hallmarks of aging. *Cell.*
643 2013;153(6):1194. doi:10.1016/j.cell.2013.05.039
- 644 4. Mizushima N, Levine B, Cuervo AM, Klionsky DJ. Autophagy fights disease through cellular self-
645 digestion. *Nature.* 2008;451(7182):1069-1075. doi:10.1038/nature06639
- 646 5. Hara T, Nakamura K, Matsui M, et al. Suppression of basal autophagy in neural cells causes
647 neurodegenerative disease in mice. *Nature.* 2006;441(7095):885-889. doi:10.1038/nature04724
- 648 6. Komatsu M, Waguri S, Chiba T, et al. Loss of autophagy in the central nervous system causes
649 neurodegeneration in mice. *Nature.* 2006;441(7095):880-884. doi:10.1038/nature04723
- 650 7. Özcan U, Cao Q, Yilmaz E, et al. Endoplasmic Reticulum Stress Links Obesity, Insulin Action, and
651 Type 2 Diabetes. *Science (80-).* 2004;306(5695):457 LP - 461.
652 <http://science.sciencemag.org/content/306/5695/457.abstract>.
- 653 8. D'Angelo MA, Raices M, Panowski SH, Hetzer MW. Age-Dependent Deterioration of Nuclear Pore
654 Complexes Causes a Loss of Nuclear Integrity in Postmitotic Cells. *Cell.* 2009;136(2):284-295.
655 doi:10.1016/j.cell.2008.11.037
- 656 9. Lane RK, Hilsabeck T, Rea SL. The role of mitochondrial dysfunction in age-related diseases.
657 *Biochim Biophys Acta - Bioenerg.* 2015;1847(11):1387-1400. doi:10.1016/j.bbabbio.2015.05.021
- 658 10. Petersen KF, Dufour S, Befroy D, Garcia R, Shulman GI. Impaired Mitochondrial Activity in the
659 Insulin-Resistant Offspring of Patients with Type 2 Diabetes. *N Engl J Med.* 2004;350(7):664-671.
660 doi:10.1056/nejmoa031314
- 661 11. Mootha VK, Lindgren CM, Eriksson KF, et al. PGC-1 α -responsive genes involved in oxidative
662 phosphorylation are coordinately downregulated in human diabetes. *Nat Genet.* 2003;34(3):267-
663 273. doi:10.1038/ng1180
- 664 12. Schapira AH V, Cooper JM, Dexter D, Clark JB, Jenner P, Marsden CD. Mitochondrial Complex I
665 Deficiency in Parkinson's Disease. *J Neurochem.* 1990;54(3):823-827. doi:10.1111/j.1471-
666 4159.1990.tb02325.x
- 667 13. Bender A, Krishnan KJ, Morris CM, et al. High levels of mitochondrial DNA deletions in substantia
668 nigra neurons in aging and Parkinson disease. *Nat Genet.* 2006;38(5):515-517.
669 doi:10.1038/ng1769
- 670 14. Wanagat J, Cao Z, Pathare P, Aiken JM. Mitochondrial DNA deletion mutations colocalize with
671 segmental electron transport system abnormalities, muscle fiber atrophy, fiber splitting, and
672 oxidative damage in sarcopenia. *FASEB J.* 2001;15(2):322-332. doi:10.1096/fj.00-0320com
- 673 15. Ashar FN, Zhang Y, Longchamps RJ, et al. Association of mitochondrial DNA copy number with
674 cardiovascular disease. *JAMA Cardiol.* 2017;2(11):1247-1255. doi:10.1001/jamacardio.2017.3683
- 675 16. Fleischman A, Makimura H, Stanley TL, et al. Skeletal muscle phosphocreatine recovery after
676 submaximal exercise in children and young and middle-aged adults. *J Clin Endocrinol Metab.*
677 2010;95(9):69-74. doi:10.1210/jc.2010-0527
- 678 17. Fannin SW, Lesnefsky EJ, Slabe TJ, Hassan MO, Hoppel CL. Aging selectively decreases oxidative
679 capacity in rat heart interfibrillar mitochondria. *Arch Biochem Biophys.* 1999;372(2):399-407.
680 doi:10.1006/abbi.1999.1508
- 681 18. Trounce I, Byrne E, Marzuki S. Decline in Skeletal Muscle Mitochondrial Respiratory Chain
682 Function: Possible Factor in Ageing. *Lancet.* 1989;333(8639):637-639. doi:10.1016/S0140-
683 6736(89)92143-0
- 684 19. Kelley DE, He J, Menshikova E V., Ritov VB. Dysfunction of mitochondria in human skeletal muscle

- 685 in type 2 diabetes. *Diabetes*. 2002;51(10):2944-2950. doi:10.2337/diabetes.51.10.2944
- 686 20. Patti ME, Butte AJ, Crunkhorn S, et al. Coordinated reduction of genes of oxidative metabolism in
687 humans with insulin resistance and diabetes: Potential role of PGC1 and NRF1. *Proc Natl Acad Sci*
688 *U S A*. 2003;100(14):8466-8471. doi:10.1073/pnas.1032913100
- 689 21. Stump CS, Short KR, Bigelow ML, Schimke JM, Nair KS. Effect of insulin on human skeletal muscle
690 mitochondrial ATP production, protein synthesis, and mRNA transcripts. *Proc Natl Acad Sci U S A*.
691 2003;100(13):7996-8001. doi:10.1073/pnas.1332551100
- 692 22. Taylor RW, Barron MJ, Borthwick GM, et al. Mitochondrial DNA mutations in human colonic crypt
693 stem cells Find the latest version : Mitochondrial DNA mutations in human colonic crypt stem
694 cells. *J Clin Invest*. 2003;112(9):1351-1360. doi:10.1172/JCI200319435.Introduction
- 695 23. Frazier AE, Thorburn DR, Compton AG. Mitochondrial energy generation disorders: Genes,
696 mechanisms, and clues to pathology. *J Biol Chem*. 2019;294(14):5386-5395.
697 doi:10.1074/jbc.R117.809194
- 698 24. Curran JE, Johnson MP, Dyer TD, et al. Genetic determinants of mitochondrial content. *Hum Mol*
699 *Genet*. 2007;16(12):1504-1514. doi:10.1093/hmg/ddm101
- 700 25. Xing J, Chen M, Wood CG, et al. Mitochondrial DNA content: Its genetic heritability and
701 association with renal cell carcinoma. *J Natl Cancer Inst*. 2008;100(15):1104-1112.
702 doi:10.1093/jnci/djn213
- 703 26. Kuan V, Denaxas S, Gonzalez-Izquierdo A, et al. A chronological map of 308 physical and mental
704 health conditions from 4 million individuals in the English National Health Service. *Lancet Digit*
705 *Heal*. 2019;1(2):e63-e77. doi:10.1016/s2589-7500(19)30012-3
- 706 27. Sudlow C, Gallacher J, Allen N, et al. UK Biobank: An Open Access Resource for Identifying the
707 Causes of a Wide Range of Complex Diseases of Middle and Old Age. *PLoS Med*. 2015;12(3):1-10.
708 doi:10.1371/journal.pmed.1001779
- 709 28. Teslovich TM, Musunuru K, Smith A V, et al. Biological, clinical and population relevance of 95 loci
710 for blood lipids. *Nature*. 2010;466(7307):707-713. <http://dx.doi.org/10.1038/nature09270>.
- 711 29. Ehret GB, Munroe PB, Rice KM, et al. Genetic variants in novel pathways influence blood pressure
712 and cardiovascular disease risk. *Nature*. 2011;478(7367):103-109. doi:10.1038/nature10405
- 713 30. Manning AK, Hivert M-F, Scott RA, et al. A genome-wide approach accounting for body mass
714 index identifies genetic variants influencing fasting glycemic traits and insulin resistance. *Nat*
715 *Genet*. 2012;44(6):659-669. <http://dx.doi.org/10.1038/ng.2274>.
- 716 31. Morris AP, Voight BF, Teslovich TM, et al. Large-scale association analysis provides insights into
717 the genetic architecture and pathophysiology of type 2 diabetes. *Nat Genet*. 2012;44(9):981-990.
718 doi:10.1038/ng.2383
- 719 32. Schunkert H, König IR, Kathiresan S, et al. Large-scale association analysis identifies 13 new
720 susceptibility loci for coronary artery disease. *Nat Genet*. 2011;43(4):333-340.
721 doi:10.1038/ng.784
- 722 33. Estrada K, Styrkarsdottir U, Evangelou E, et al. Genome-wide meta-analysis identifies 56 bone
723 mineral density loci and reveals 14 loci associated with risk of fracture. *Nat Genet*.
724 2012;44(5):491-501. doi:10.1038/ng.2249
- 725 34. Christophersen IE, Rienstra M, Roselli C, et al. Large-scale analyses of common and rare variants
726 identify 12 new loci associated with atrial fibrillation. *Nat Genet*. 2017;49(6):946-952.
727 doi:10.1038/ng.3843
- 728 35. Pattaro C, Teumer A, Gorski M, et al. Genetic associations at 53 loci highlight cell types and
729 biological pathways relevant for kidney function. *Nat Commun*. 2016;7:1-19.
730 doi:10.1038/ncomms10023
- 731 36. Nalls MA, Blauwendraat C, Vallerga CL, et al. Identification of novel risk loci, causal insights, and
732 heritable risk for Parkinson's disease: a meta-analysis of genome-wide association studies. *Lancet*

- 733 *Neurol.* 2019;18(12):1091-1102. doi:10.1016/S1474-4422(19)30320-5
- 734 37. Lambert JC, Ibrahim-Verbaas CA, Harold D, et al. Meta-analysis of 74,046 individuals identifies 11
735 new susceptibility loci for Alzheimer's disease. *Nat Genet.* 2013;45(12):1452-1458.
736 doi:10.1038/ng.2802
- 737 38. Finucane HK, Bulik-Sullivan B, Gusev A, et al. Partitioning heritability by functional annotation
738 using genome-wide association summary statistics. *Nat Genet.* 2015;47(11):1228-1235.
739 doi:10.1038/ng.3404
- 740 39. Bulik-Sullivan B, Finucane HK, Anttila V, et al. An atlas of genetic correlations across human
741 diseases and traits. *Nat Genet.* 2015;47(11):1236-1241. doi:10.1038/ng.3406
- 742 40. Wasmer K, Eckardt L, Breithardt G. Predisposing factors for atrial fibrillation in the elderly. *J*
743 *Geriatr Cardiol.* 2017;14(3):179-184. doi:10.11909/j.issn.1671-5411.2017.03.010
- 744 41. Calvo SE, Clauser KR, Mootha VK. MitoCarta2.0: An updated inventory of mammalian
745 mitochondrial proteins. *Nucleic Acids Res.* 2016;44(D1):D1251-D1257. doi:10.1093/nar/gkv1003
- 746 42. MacArthur J, Bowler E, Cerezo M, et al. The new NHGRI-EBI Catalog of published genome-wide
747 association studies (GWAS Catalog). *Nucleic Acids Res.* 2016;45(November 2016):gkw1133.
748 doi:10.1093/nar/gkw1133
- 749 43. Finucane HK, Reshef YA, Anttila V, et al. Heritability enrichment of specifically expressed genes
750 identifies disease-relevant tissues and cell types. *Nat Genet.* 2018;50(4):621-629.
751 doi:10.1038/s41588-018-0081-4
- 752 44. de Leeuw CA, Mooij JM, Heskes T, Posthuma D. MAGMA: Generalized Gene-Set Analysis of GWAS
753 Data. *PLoS Comput Biol.* 2015;11(4):1-19. doi:10.1371/journal.pcbi.1004219
- 754 45. Yamamoto K, Sakaue S, Matsuda K, et al. Genetic and phenotypic landscape of the mitochondrial
755 genome in the Japanese population. *Commun Biol.* 2020;3(1):104. doi:10.1038/s42003-020-0812-
756 9
- 757 46. Binder JX, Pletscher-Frankild S, Tsafou K, et al. COMPARTMENTS: Unification and visualization of
758 protein subcellular localization evidence. *Database.* 2014;2014:1-9.
759 doi:10.1093/database/bau012
- 760 47. Carbon S, Douglass E, Dunn N, et al. The Gene Ontology Resource: 20 years and still GOing
761 strong. *Nucleic Acids Res.* 2019;47(D1):D330-D338. doi:10.1093/nar/gky1055
- 762 48. Ashburner M, Ball CA, Blake JA, et al. Gene Ontology: Tool for The Unification of Biology. *Nat*
763 *Genet.* 2000;25(1):25-29. doi:10.1038/75556
- 764 49. Lambert SA, Jolma A, Campitelli LF, et al. The Human Transcription Factors. *Cell.* 2018;172(4):650-
765 665. doi:10.1016/j.cell.2018.01.029
- 766 50. Kapopoulou A, Mathew L, Wong A, Trono D, Jensen JD. The evolution of gene expression and
767 binding specificity of the largest transcription factor family in primates. *Evolution (N Y).*
768 2016;70(1):167-180. doi:10.1111/evo.12819
- 769 51. Timmers PRHJ, Mounier N, Lall K, et al. Genomics of 1 million parent lifespans implicates novel
770 pathways and common diseases and distinguishes survival chances. *Elife.* 2019;8:1-40.
771 doi:10.7554/elife.39856
- 772 52. Zenin A, Tsepilov Y, Sharapov S, et al. Identification of 12 genetic loci associated with human
773 healthspan. *Commun Biol.* 2019;2(1). doi:10.1038/s42003-019-0290-0
- 774 53. Jimenez-Sanchez G, Childs B, Valle D. Human Disease Genes. *Nature.* 2001;409:853-855.
- 775 54. Worman HJ, Courvalin JC. The nuclear lamina and inherited disease. *Trends Cell Biol.*
776 2002;12(12):591-598. doi:10.1016/S0962-8924(02)02401-7
- 777 55. Cleaver JE. It was a very good year for DNA repair. *Cell.* 1994;76(1):1-4. doi:10.1016/0092-
778 8674(94)90165-1
- 779 56. Karczewski KJ, Francioli LC, Tiao G, et al. The mutational constraint spectrum quantified from
780 variation in 141,456 humans. *Nature.* 2020;581(7809):434-443. doi:10.1038/s41586-020-2308-7

- 781 57. Colacurcio DJ, Nixon RA. Disorders of lysosomal acidification—The emerging role of v-ATPase in
782 aging and neurodegenerative disease. *Ageing Res Rev.* 2016;32:75-88.
783 doi:10.1016/j.arr.2016.05.004
- 784 58. Kanfi Y, Peshti V, Gil R, et al. SIRT6 protects against pathological damage caused by diet-induced
785 obesity. *Ageing Cell.* 2010;9(2):162-173. doi:10.1111/j.1474-9726.2009.00544.x
- 786 59. Blasco MA. Telomere length, stem cells and aging. *Nat Chem Biol.* 2007;3(10):640-649.
787 doi:10.1038/nchembio.2007.38
- 788 60. Bhattarai KR, Chaudhary M, Kim H-R, Chae H-J. Endoplasmic Reticulum (ER) Stress Response
789 Failure in Diseases. *Trends Cell Biol.* 2020;xx(xx):5-7. doi:10.1016/j.tcb.2020.05.004
- 790 61. De Leeuw CA, Neale BM, Heskes T, Posthuma D. The statistical properties of gene-set analysis.
791 *Nat Rev Genet.* 2016;17(6):353-364. doi:10.1038/nrg.2016.29
- 792 62. Loh PR, Bhatia G, Gusev A, et al. Contrasting genetic architectures of schizophrenia and other
793 complex diseases using fast variance-components analysis. *Nat Genet.* 2015;47(12):1385-1392.
794 doi:10.1038/ng.3431
- 795 63. Billingsley KJ, Barbosa IA, Bandrés-Ciga S, et al. Mitochondria function associated genes
796 contribute to Parkinson's Disease risk and later age at onset. *npj Park Dis.* 2019;5(1).
797 doi:10.1038/s41531-019-0080-x
- 798 64. Kraja AT, Liu C, Fetterman JL, et al. Associations of Mitochondrial and Nuclear Mitochondrial
799 Variants and Genes with Seven Metabolic Traits. *Am J Hum Genet.* 2019;104(1):112-138.
800 doi:10.1016/j.ajhg.2018.12.001
- 801 65. Xue A, Wu Y, Zhu Z, et al. Genome-wide association analyses identify 143 risk variants and
802 putative regulatory mechanisms for type 2 diabetes. *Nat Commun.* 2018;9(1).
803 doi:10.1038/s41467-018-04951-w
- 804 66. Jansen IE, Savage JE, Watanabe K, et al. Genome-wide meta-analysis identifies new loci and
805 functional pathways influencing Alzheimer's disease risk. *Nat Genet.* 2019;51(3):404-413.
806 doi:10.1038/s41588-018-0311-9
- 807 67. Pardiñas AF, Holmans P, Pocklington AJ, et al. Common schizophrenia alleles are enriched in
808 mutation-intolerant genes and in regions under strong background selection. *Nat Genet.*
809 2018;50(3):381-389. doi:10.1038/s41588-018-0059-2
- 810 68. Maurano MT, Humbert R, Rynes E, et al. Systematic localization of common disease-associated
811 variation in regulatory DNA. *Science (80-).* 2012;337(6099):1190-1195.
812 doi:10.1126/science.1222794
- 813 69. Raule N, Sevini F, Santoro A, Altiglia S, Franceschi C. Association studies on human mitochondrial
814 DNA: Methodological aspects and results in the most common age-related diseases.
815 *Mitochondrion.* 2007;7(1-2):29-38. doi:10.1016/j.mito.2006.11.013
- 816 70. Yu X, Koczan D, Sulonen AM, et al. mtDNA nt13708A variant increases the risk of multiple
817 sclerosis. *PLoS One.* 2008;3(2):1-7. doi:10.1371/journal.pone.0001530
- 818 71. Hudson G, Nalls M, Evans JR, et al. Two-stage association study and meta-analysis of
819 mitochondrial DNA variants in Parkinson disease. *Neurology.* 2013;80(22):2042-2048.
820 doi:10.1212/WNL.0b013e318294b434
- 821 72. Samuels DC, Carothers AD, Horton R, Chinnery PF. The power to detect disease associations with
822 mitochondrial DNA haplogroups. *Am J Hum Genet.* 2006;78(4):713-720. doi:10.1086/502682
- 823 73. Biffi A, Anderson CD, Nalls MA, et al. Principal-Component Analysis for Assessment of Population
824 Stratification in Mitochondrial Medical Genetics. *Am J Hum Genet.* 2010;86(6):904-917.
825 doi:10.1016/j.ajhg.2010.05.005
- 826 74. Segrè A V, Consortium D, investigators M, et al. Common Inherited Variation in Mitochondrial
827 Genes Is Not Enriched for Associations with Type 2 Diabetes or Related Glycemic Traits. *PLOS*
828 *Genet.* 2010;6(8):e1001058. <https://doi.org/10.1371/journal.pgen.1001058>.

- 829 75. Saxena R, De Bakker PIW, Singer K, et al. Comprehensive association testing of common
830 mitochondrial DNA variation in metabolic disease. *Am J Hum Genet.* 2006;79(1):54-61.
831 doi:10.1086/504926
- 832 76. Hudson G, Gomez-Duran A, Wilson IJ, Chinnery PF. Recent Mitochondrial DNA Mutations
833 Increase the Risk of Developing Common Late-Onset Human Diseases. *PLoS Genet.* 2014;10(5).
834 doi:10.1371/journal.pgen.1004369
- 835 77. Hudson G, Panoutsopoulou K, Wilson I, et al. No evidence of an association between
836 mitochondrial DNA variants and osteoarthritis in 7393 cases and 5122 controls. *Ann Rheum Dis.*
837 2013;72(1):136-139. doi:10.1136/annrheumdis-2012-201932
- 838 78. Seidman JG, Seidman C. Transcription factor haploinsufficiency: When half a loaf is not enough. *J*
839 *Clin Invest.* 2002;109(4):451-455. doi:10.1172/JCI0215043
- 840 79. Lee R Van Der, Correard S, Wasserman WW. Deregulated Regulators : Disease-Causing cis
841 Variants in Transcription Factor Genes. *Trends Genet.* 2020;xx(xx). doi:10.1016/j.tig.2020.04.006
- 842 80. Wright S. Physiological and Evolutionary Theories of Dominance. *Am Nat.* 1934;68(714):24.
- 843 81. Kacser H, Burns JA. The molecular basis of dominance. *Genetics.* 1981;97(3-4):639-666.
- 844 82. Chance B, Williams GR. RESPIRATORY ENZYMES IN OXIDATIVE PHOSPHORYLATION: III. THE
845 STEADY STATE. *J Biol Chem.* 1955;217(1):409-428. <http://www.jbc.org/content/217/1/409.short>.
- 846 83. Vafai SB, Mootha VK. Mitochondrial disorders as windows into an ancient organelle. *Nature.*
847 2012;491(7424):374-383. doi:10.1038/nature11707
- 848 84. Balaban RS, Kantor HL, Katz LA, Briggs RW. Relation between work and phosphate metabolite in
849 the in vivo paced mammalian heart. *Science (80-).* 1986;232(4754):1121-1123.
850 doi:10.1126/science.3704638
- 851 85. To TL, Cuadros AM, Shah H, et al. A Compendium of Genetic Modifiers of Mitochondrial
852 Dysfunction Reveals Intra-organelle Buffering. *Cell.* 2019;179(5):1222-1238.e17.
853 doi:10.1016/j.cell.2019.10.032
- 854 86. Golan D, Lander ES, Rosset S. Measuring missing heritability: Inferring the contribution of
855 common variants. *Proc Natl Acad Sci U S A.* 2014;111(49):E5272-E5281.
856 doi:10.1073/pnas.1419064111
- 857 87. Polderman TJC, Benyamin B, De Leeuw CA, et al. Meta-analysis of the heritability of human traits
858 based on fifty years of twin studies. *Nat Genet.* 2015;47(7):702-709. doi:10.1038/ng.3285
- 859 88. Fuchsberger C, Flannick J, Teslovich TM, et al. The genetic architecture of type 2 diabetes.
860 *Nature.* 2016;536(7614):41-47. doi:10.1038/nature18642
- 861 89. Hill WG, Goddard ME, Visscher PM. Data and theory point to mainly additive genetic variance for
862 complex traits. *PLoS Genet.* 2008;4(2). doi:10.1371/journal.pgen.1000008
- 863 90. Zhu Z, Bakshi A, Vinkhuyzen AAE, et al. Dominance genetic variation contributes little to the
864 missing heritability for human complex traits. *Am J Hum Genet.* 2015;96(3):377-385.
865 doi:10.1016/j.ajhg.2015.01.001
- 866 91. Rand DM, Mossman JA. Mitonuclear conflict and cooperation govern the integration of
867 genotypes, phenotypes and environments. *Philos Trans R Soc B Biol Sci.* 2020;375(1790).
868 doi:10.1098/rstb.2019.0188
- 869 92. Sackton TB, Hartl DL. Genotypic Context and Epistasis in Individuals and Populations. *Cell.*
870 2016;166(2):279-287. doi:10.1016/j.cell.2016.06.047
- 871 93. Hemani G, Shakhbazov K, Westra HJ, et al. Detection and replication of epistasis influencing
872 transcription in humans. *Nature.* 2014;508(7495):249-253. doi:10.1038/nature13005
- 873 94. Solenski NJ, DiPierro CG, Trimmer PA, Kwan AL, Helms GA. Ultrastructural changes of neuronal
874 mitochondria after transient and permanent cerebral ischemia. *Stroke.* 2002;33(3):816-824.
875 doi:10.1161/hs0302.104541
- 876 95. Flameng W, Andres J, Ferdinande P, Mattheussen M, Van Belle H. Mitochondrial function in

- 877 myocardial stunning. *J Mol Cell Cardiol.* 1991;23(1):1-11. doi:10.1016/0022-2828(91)90034-J
878 96. Weinbrenner C, Liu GS, Downey JM, Cohen M V. Cyclosporine a limits myocardial infarct size
879 even when administered after onset of ischemia. *Cardiovasc Res.* 1998;38(3):676-684.
880 doi:10.1016/S0008-6363(98)00064-9
881 97. Kubben N, Misteli T. Shared molecular and cellular mechanisms of premature ageing and ageing-
882 associated diseases. *Nat Rev Mol Cell Biol.* 2017;18(10):595-609. doi:10.1038/nrm.2017.68
883 98. Garcia CK, Wright WE, Shay JW. Human diseases of telomerase dysfunction: Insights into tissue
884 aging. *Nucleic Acids Res.* 2007;35(22):7406-7416. doi:10.1093/nar/gkm644
885 99. Han S, Brunet A. Histone methylation makes its mark on longevity. *Trends Cell Biol.*
886 2012;22(1):42-49. doi:10.1016/j.tcb.2011.11.001
887 100. Bahar R, Hartmann CH, Rodrigue KA, et al. Increased cell-to-cell variation in gene expression in
888 ageing mouse heart. *Nature.* 2006;441(7096):1011-1014. doi:10.1038/nature04844
889 101. Kanfi Y, Naiman S, Amir G, et al. The sirtuin SIRT6 regulates lifespan in male mice. *Nature.*
890 2012;483(7388):218-221. doi:10.1038/nature10815
891 102. Karczewski KJ, Dudley JT, Kukurba KR, et al. Systematic functional regulatory assessment of
892 disease-associated variants. *Proc Natl Acad Sci U S A.* 2013;110(23):9607-9612.
893 doi:10.1073/pnas.1219099110
894 103. Yanai I, Benjamin H, Shmoish M, et al. Genome-wide midrange transcription profiles reveal
895 expression level relationships in human tissue specification. *Bioinformatics.* 2005;21(5):650-659.
896 doi:10.1093/bioinformatics/bti042
897 104. Melé M, Ferreira PG, Reverter F, et al. The human transcriptome across tissues and individuals.
898 *Science (80-).* 2015;348(6235):660-665. <http://dx.doi.org/10.1126/science.aaa0355>.
899 105. Morris JA, Randall JC, Maller JB, Barrett JC. Evoker: A visualization tool for genotype intensity
900 data. *Bioinformatics.* 2010;26(14):1786-1787. doi:10.1093/bioinformatics/btq280
901 106. Yates AD, Achuthan P, Akanni W, et al. Ensembl 2020. *Nucleic Acids Res.* 2020;48(D1):D682-D688.
902 doi:10.1093/nar/gkz966
903 107. Litman T, Stein WD. Obtaining estimates for the ages of all the protein-coding genes and most of
904 the ontology-identified noncoding genes of the human genome, assigned to 19 phylostrata.
905 *Semin Oncol.* 2019;46(1):3-9. doi:10.1053/j.seminoncol.2018.11.002
906